Ultrasonic-Assisted Fabrication of MIL-100(Fe) Metal–Organic Frameworks as a Carrier for the Controlled Delivery of the Chloroquine Drug

Bac Thanh Le, Duong Duc La, and Phuong Thi Hoai Nguyen*

ACCESS | Metrics & More | Article Recommendations | SI Supporting Information

ABSTRACT: Metal–organic framework materials (MOFs) are materials with an ordered crystalline structure and high porosity that have been intensively investigated for many applications, such as gas adsorption, catalysis, sensors, drug delivery, and so on. Among them, the MOF-based drug delivery system has received increasing interest from scientists worldwide. This work presented the preparation of the MIL-100(Fe) metal–organic framework from the organic ligand of trimesic acid and iron ions with ultrasonic assistance. Scanning electron microscopy (SEM), Brunauer–Emmett–Teller surface area (BET), X-ray diffraction (XRD), infrared spectroscopy (FTIR), and Raman spectroscopy were employed to characterize the prepared MIL-100(Fe) material. MIL-100(Fe) materials synthesized by the ultrasonic method have uniform particle morphology ranging from 100 to 300 nm with a surface area of 1033 m^2/ g. The prepared MIL-100(Fe) was employed as a carrier for delivering chloroquine drug with a maximal loading capacity of 220 mg/g. The MIL-100(Fe)@chloroquine system was also characterized in detail. The delivery system's slow drug release was studied, showing that nearly 80% of chloroquine molecules were released after 7.5 h of immersing time in PBS and simulated gastric solutions and completely detached from the MIL-100(Fe)@chloroquine system only after approximately 80 h. This result shows the ability to control chloroquine drug release of the material, reducing the possibility of drug shock.
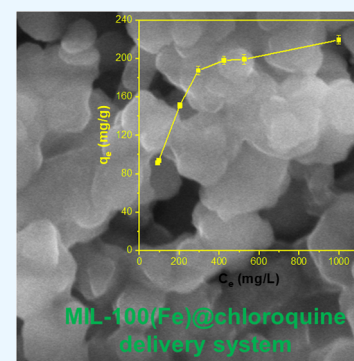
1. INTRODUCTION

In recent years, metal–organic framework materials (MOFs) have attracted significant attention from researchers due to their high surface area, small particle size, and novel physical and chemical properties with controllable functional groups.[1−3] MOF materials have been applied in many fields, including, but not limited to, environmental treatment, gas sensing, catalysis, medicine, and pharmacy.[4−9] Among them, the application of MOFs as drug carriers is increasingly attractive worldwide.[10−13] To be effective in drug delivery, MOF materials should have unique properties such as high porosity,[14] high stability,[15] good degradability, and biocompatibility.[16] One of the most studied MOFs families in medical applications is the iron-based MOF, with high porosity, reasonable stable, good biodegradability, and biocompatibility.[7,17,18] Many approaches could be utilized to synthesize iron-based MOFs such as hydrothermal, reflux, microwave, and ultrasonic methods.[7,19−23] Among them, the ultrasonic method is a simple method with a fast synthesis time, user-friendliness, good performance, and low energy consumption. Additionally, the use of green solvents such as water and ethanol makes the ultrasonic method one of the green methods for the fabrication of MOF materials.

Chloroquine is an active drug usually used for treating rheumatism, lupus erythematosus, and malaria. Chloroquine is usually utilized in the form of phosphate or sulfate with the chemical formula $C_{18}H_{26}ClN_3 \cdot 2H_3PO_4$ or $C_{18}H_{26}ClN_3 \cdot H_2SO_4$[24,25] Recently, some preliminary reports suggest the employment of chloroquine in the treatment of viruses and symptoms of patients infected with SARS-CoV-2.[26,27] However, when using chloroquine in the form of phosphate or sulfate, the drug is absorbed very quickly with a low safety limit; thus, it can easily lead to an overdose with many side effects on other organs. After oral administration, the drug is released in the stomach and intestines and permeates to the intestinal wall, highly concentrated in leukocytes, and concentrations in spleens, and liver. Due to the rapid absorption of the drug, the metabolism is slow, resulting in an increase in peak serum concentrations soon after oral administration, predisposing to symptoms of overdose.[28,29]

To avoid the side effects of using an overdose of chloroquine, several nanomaterials have been employed to control the release of this drug.[30−33] Among these, MOF nanomaterials have been recently considered effective carriers for the controlled delivery of the chloroquine drug.[34−37] For
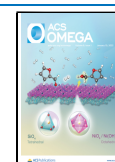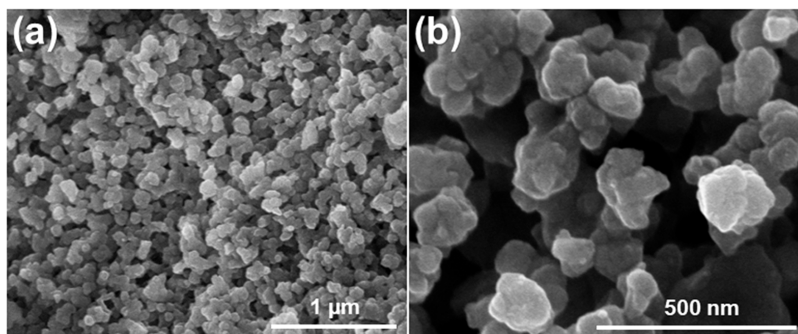
Figure 1. Scanning electron micrograph of MIL-100(Fe) metal−organic frameworks at 30.000 (a) and 100.000 magnifications (b).
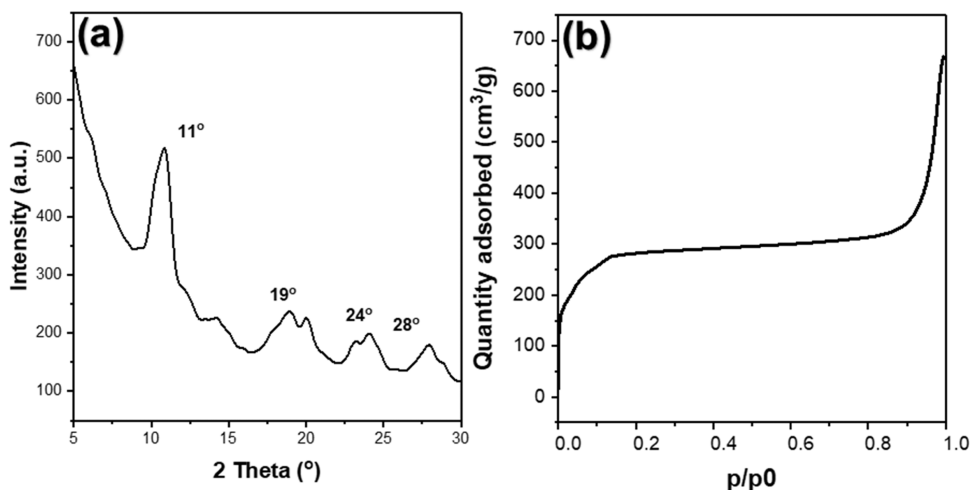

Figure 2. (a) XRD pattern and (b) nitrogen adsorption plot of MIL-100(Fe) metal−organic frameworks.

example, Shi's group successfully encapsulated a special cancer cells identifier of methoxy poly(ethylene glycol)-folate (FA-PEG) in the chloroquine@ZIF-8 (zeolitic imidazolate framework) to form FA-PEG/chloroquine@ZIF-8.[38] The prepared delivery system revealed controlled delivery of the chloroquine and enhanced the autophagy inhibiting efficiency. The UiO-66 metal−organic framework was also successfully fabricated and used as a potential carrier for chloroquine delivery.[39] The result showed that the obtained chloroquine@UiO-66 delivery system significantly reduced the release speed of chloroquine compared to the pristine drug. Recently, Zhang et al. reported the fabrication of titanium-based MOFs for the delivery of chloroquine drug.[40] The resultant Ti-based MOFs reveal high loading capacity with the slow release of chloroquine, with 70% of the drug released after 13 days in the PBS solution. However, to the best of our knowledge, the use of iron-based MOFs for the controlled delivery of chloroquine drug have not been studied.

Herein, we report a facile approach to fabricating MIL-100(Fe) iron-based MOFs with the assistance of ultrasonic conditions for potential application as a controlled carrier for chloroquine delivery. The MIL-100(Fe) and MIL-100(Fe)@ chloroquine delivery systems are well-characterized by SEM, FTIR, XRD, Raman, and BET techniques. The loading and drug-releasing behaviors of the MIL-100(Fe)@chloroquine delivery system are also investigated in detail.

2. RESULTS AND DISCUSSION

Characterizations of MIL-100(Fe). The surface morphologies of the MIL-100(Fe) metal−organic frameworks were observed using a scanning electron microscope, as shown in Figure 1. The prepared framework has an irregular shape with particles size ranging from 100 to 300 nm and tends to aggregate into large particles. The particle size of MIL-100(Fe) obtained in this paper is smaller than that of MIL-100(Fe) materials reported previously. The small size of MIL-100(Fe) can be explained by the ultrasonic-assisted synthesis process and a short reaction time (less than 10 min), in which the ultrasonic wave plays the role of a dispersing agent that hinders the development of the particle's size.

The crystallinity of the material was investigated using XRD techniques. The result is exhibited in Figure 2a. The XRD pattern shows characteristic peaks at 11, 19, 24, and 28°, which are consistent with characteristic peaks in the XRD pattern of simulated MIL-100(Fe).[7,41,42] The broadening of the diffraction peaks of the prepared materials was attributed to the ultrasonic process, which limits the crystal growth and crystallinity of the material. Additionally, the synthesis media is water, forming on the crystals of insoluble organic acids (heterogeneous reaction), which resulted in a different crystallinity from the material formed from homogeneous crystallization. The surface area is one of the important properties of MOF materials. In this work, the prepared MIL-100(Fe)material's surface area was evaluated by nitrogen isothermal adsorption (Figure 2b). The result reveals that the material has a high surface area of 1033 m²/g with a pore
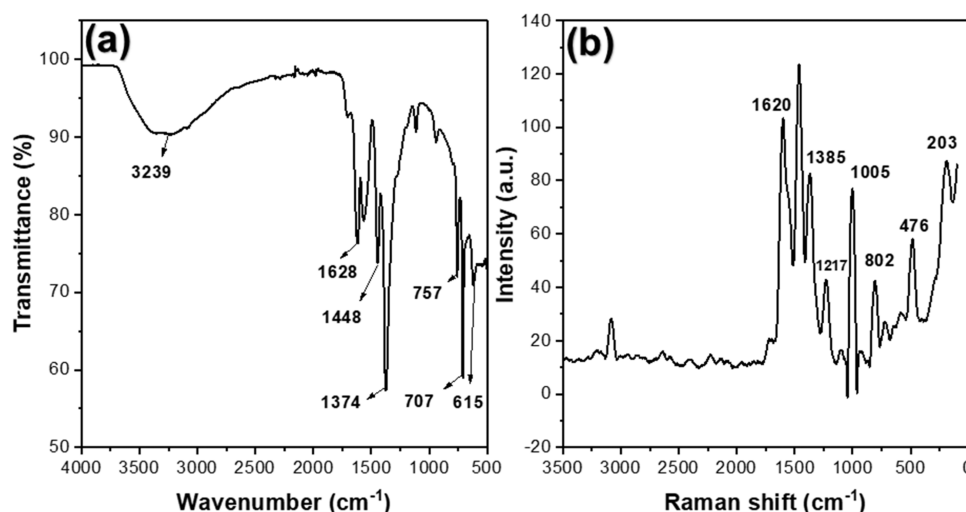
Figure 3. (a) FTIR spectrum and (b) Raman spectrum of MIL-100(Fe) metal−organic frameworks.

diameter of 2.96 nm and a pore volume of 0.764 cm^3/g. The surface area of MIL-100(Fe) prepared using the ultra-sonication method in an aqueous solution is higher than that of other MIL-100(Fe) reported previously.[19,43,44] The larger pore diameter of MIL-100(Fe) material compared to previous studies could be explained by ultrasonic assistance during the synthesizing process.[7] These porous properties of the material could be suitable for drug delivery applications.

FTIR and Raman spectroscopies were employed to study the chemical bonds and structure of the materials (Figure 3). As shown in Figure 3a, the FTIR spectrum reveals stretching vibration at approximately 3239 cm^{-1} due to the O−H elongation stretching group in MIL-100(Fe) and moisture from the environment. The vibration band at the wavenumber of 1628 cm^{-1} belongs to the C=O bending of the carboxylate groups. The characteristic peaks at 1448 and 1374 cm^{-1} are assigned to the symmetric and asymmetric vibrations of the COO− group. The C−H bonding of the benzene ring in MIL-100(Fe) is also observed at the vibration bands 757 and 70 cm^{-1}.[45,46] Additionally, the band observed at 615 cm^{-1} corresponds to the Fe−O stretching vibrations, demonstrating the presence of Fe in the framework of MIL-100(Fe).[47] The result further confirms the successful formation of MIL-100(Fe) metal−organic framework trimesic acid−organic bonds and metal ions. The other interference peaks with relatively low intensity are also observed in the FTIR spectrum, which is ascribed to the small amount of H$_3$BTC acid residual remaining in the activity of the material's framework.

The analysis results on the Raman spectrum also gave similar results (Figure 3b). The Raman shifts in the range of 203−476 cm^{-1} are due to the presence of Fe ions in the lattice of MIL-100(Fe). The bands at 802 and 1005 cm^{-1} belong to the benzene ring oscillations in the BTC molecules. The peak that appeared at 1217 cm^{-1} is ascribed to the C−O−Fe bonding of the iron trimer, and the peaks ranging from 1385 to 1620 cm^{-1} are assigned to the H−OH bond in the water molecules.[48]

Chloroquine Loading and Releasing. With a surface area of 1033 m^2/g, a pore diameter of 2.96 nm, a pore volume of 0.764 cm^3/g, and especially the presence of functional groups in the network, prepared MIL-100(Fe) could be effectively employed as a carrier for the drug delivery system. This work studied the capability of the prepared material for the loading and release of chloroquine drugs. At first, the

adsorption (loading) kinetics was investigated for the loading of chloroquine by the material at a drug concentration of 100 ppm, and the result is shown in Figure 4. It is obvious that the
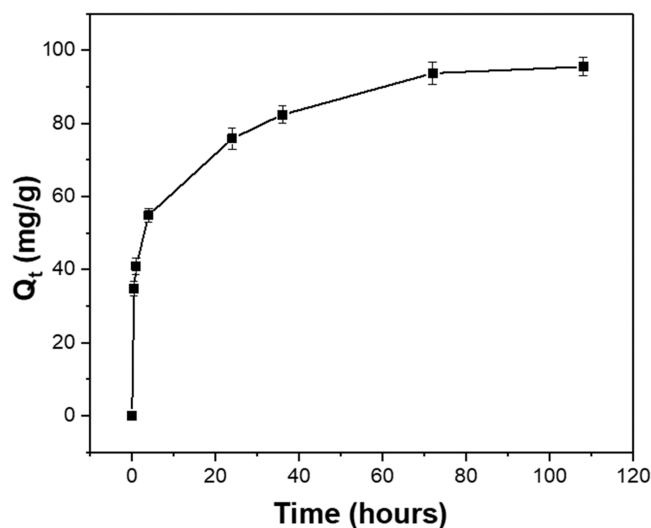

Figure 4. Loading kinetics of chloroquine drug by MIL-100(Fe) metal−organic frameworks.

loading time greatly affects the loading capacity of MIL-100(Fe). Fifty percent of the chloroquine drug was loaded on the material only after 5 h of immersing time. The loading capacities gradually increased and reached an equilibrium state after 120 h. Thus, the immersing time of 120 h was selected as the loading time for chloroquine by MIL-100(Fe).

The carrier's maximal loading capacity is essential to evaluate the possibility of materials used for drug delivery systems. This work investigated the loading capacity of prepared MIL-100(Fe) for chloroquine drug by studying the adsorption isotherm of material at different chloroquine concentrations at the equilibrium point. The result is shown in Figure 5a. It can be seen that the loading capacity increases along with the increase in drug concentrations. The drug adsorption by the material sharply increased with concentrations of lower than 300 ppm. At a concentration of higher than 300 ppm, the drug loading capacity slowly increased and
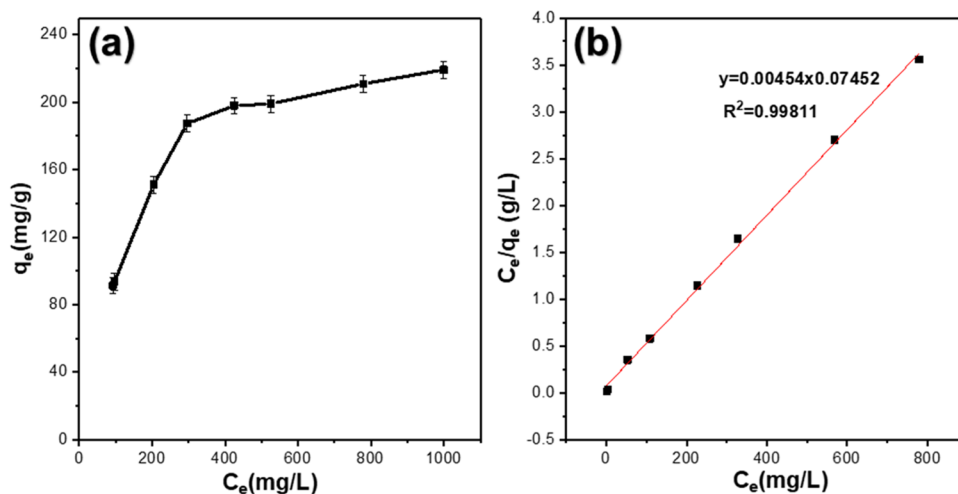
Figure 5. (a) Dependence of the loading capacity on the initial chloroquine concentration and (b) adsorption isotherm of MIL-100(Fe) metal—organic frameworks for chloroquine drug.

gradually reached the adsorption equilibrium state of the material. To determine the maximal loading capacity of the material for the chloroquine drug, the Langmuir isotherm model was plotted, as shown in Figure 5b. From the Langmuir plot, the maximal loading capacity of MIL-100(Fe) for chloroquine drug was calculated to be around Q_{max} = 220 mg/g, which is higher than those of other MOF materials used for loading of chloroquine such as ZIF-8 (180 mg/g)[38] and UiO-66 (21.28 mg/g).[39] This loading capacity is reasonable for employing MIL-100(Fe) metal—organic framework as a carrier system for chloroquine delivery.

Illustrated in Figure 6 are the FTIR spectra of pure chloroquine, MIL-100(Fe), and MIL-100(Fe) systems, which
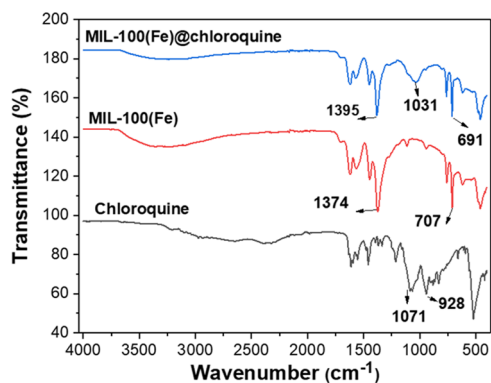

Figure 6. FTIR spectra of the chloroquine (black line) and MIL-100(Fe) before (red line) and after (blue line) loading with chloroquine.

is used to confirm the presence of chloroquine in the structure of the material. The FTIR spectrum of the MIL-100(Fe)@chloroquine system shows all of the characteristic peaks of MIL-100(Fe), which was analyzed in the previous section. The delivery system also exhibits the characteristic FTIR peaks of chloroquine compared to that of pristine chloroquine. Interestingly, the shift in the vibration bands at 1374 cm^{-1} of MIL-100(Fe) and at 1071 cm^{-1} of chloroquine compared to the FTIR spectrum of MIL-100(Fe)@chloroquine demonstrates the bonding between the material and drug.

The successful chloroquine loading by MIL-100(Fe) was further confirmed by SEM image, XRD pattern, and nitrogen adsorption plot (Figure 7). It can be obvious from Figure 7a,b that the surface morphology of the material after chloroquine loading negligibly changed from the morphology of the pristine MIL-100(Fe) before drug loading. The SEM images show that the outer surface of the MIL-100(Fe)@chloroquine system has a translucent coating, which is ascribed to the attachment of the chloroquine molecules to the surface of MIL-100(Fe). This result agrees with the XRD pattern of MIL-100(Fe)@chloroquine (Figures 7c and S1). The X-ray pattern shows that MIL-100(Fe) after carrying chloroquine has the same diffraction peaks as that of pristine MIL-100(Fe); however, the intensity is significantly decreased. This can be explained by the presence of an amorphous chloroquine molecule in the framework of MIL-100(Fe), which reduces the crystallinity of the MIL-100(Fe)@chloroquine system. The BET surface area and pore volume significantly reduce from 1033.7 m^2/g and 0.76 cm^3/g to 89.48 m^2/g and 0.35 cm^3/g for the MIL-100(Fe) material before and after loading with chloroquine, respectively. This is evidence of the successful integration in the pores of MIL-100(Fe); as a result, the porosity of the MIL-100(Fe)@chloroquine system remarkably reduces.

To evaluate the drug release ability of the MIL-100(Fe)@chloroquine system, the loaded materials were immersed into PBS (pH of 7.4) and simulated gastric pH solution (pH of 2) at a temperature of 37 °C. Figure 8 shows the chloroquine release percentage as a function of time in PBS and simulated gastric pH solution. It has been demonstrated that the MOF delivery system reveals two releasing steps for the loaded drug. In the first step, a drug with weak interaction with the MOF material is released into the free molecules. The second step is releasing the drug with strong bonding within the network of the MOF material. The prepared MIL-100(Fe)@chloroquine system in this work also showed two stages of chloroquine drug release. The first stage is the release of free chloroquine molecules or weakly bound drugs on the surface of MIL-100(Fe) material with a release percentage of 15—20% in the first 30 min and reaching nearly 80% after 7.5 h of immersing time. The releasing speed in pH 2 was faster than that of the PBS solution. In the later stage, the remaining drug with a solid bond to the MIL-100(Fe) network was slowly released and only completely detached from the material after 80 h.[49] In this
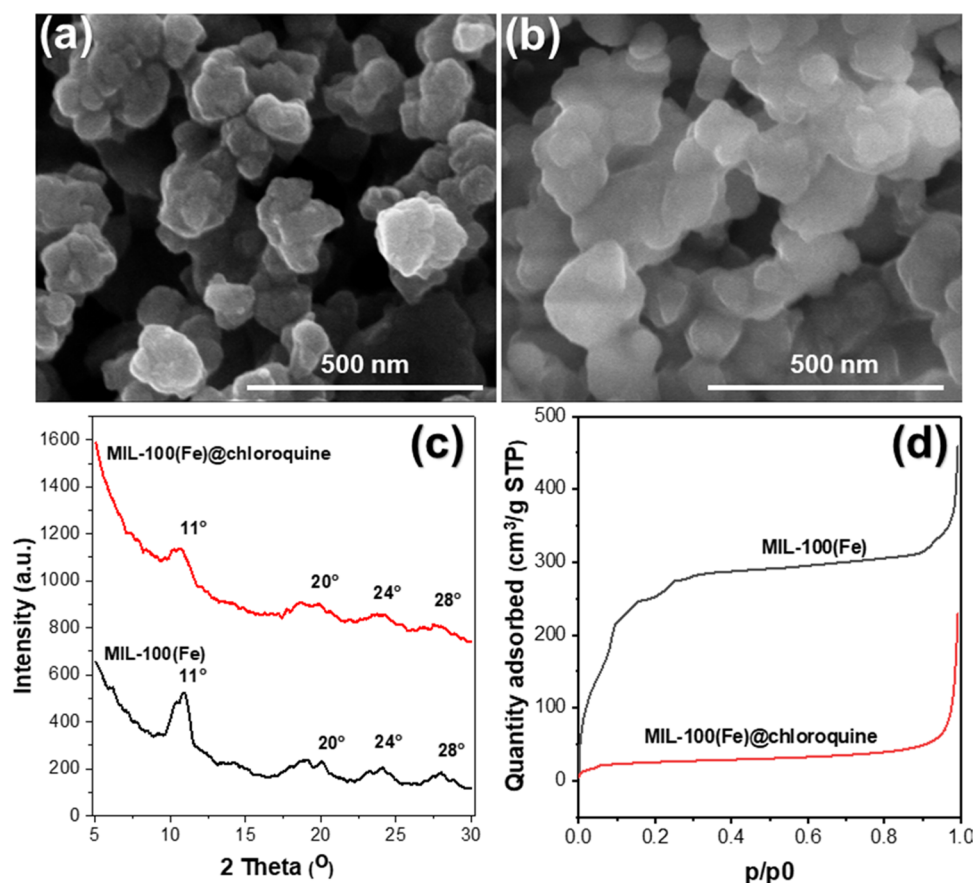
Figure 7. Scanning electron micrograph of MIL-100(Fe) (a) before and (b) after loading with chloroquine drug. (c) XRD pattern and (d) nitrogen adsorption plot of the MIL-100(Fe)@chloroquine system.
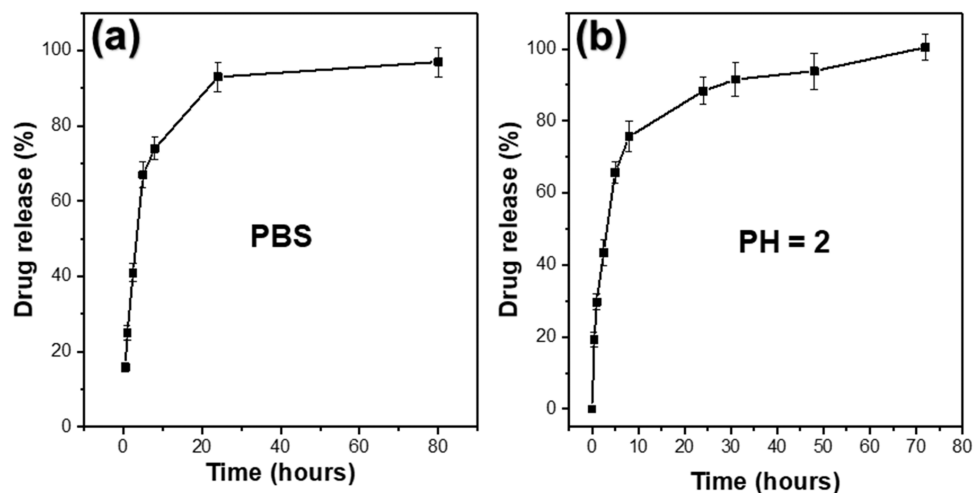

Figure 8. Release of chloroquine from MIL-100(Fe)@chloroquine system (a) in PBS and (b) in pH 2.

releasing stage, the chloroquine molecules diffused from inside of MIL-100(Fe) network into the solution, and at the end of the stage, the structural material was observed to be collapsed. This result is much slower than using the commercial chloroquine-containing drug with 100% release after 2 h.

The XRD patterns of the MIL-100(Fe)@chloroquine system after releasing chloroquine in PBS and pH 2 are studied as shown in Figure 9a. It can be seen that the diffraction peaks of the MIL-100(Fe) XRD pattern after the release of chloroquine in the PBS solution is negligible

decrease, demonstrating the robustness of MIL-100(Fe) metal−organic frameworks in the PBS media. In contrast, the XRD pattern of MIL-100(Fe) after releasing chloroquine in the pH 2 solution shows a significant reduction of characteristic diffraction peaks of the MIL-100(Fe) material, indicating the degradation of material in the pH 2 solution. These results were further evident by the BET analysis with the surface areas of the MIL-100(Fe) metal−organic frameworks after releasing chloroquine in PBS and the pH 2 solutions determined to be 917.9 and 585.3 m^2/g, respectively,
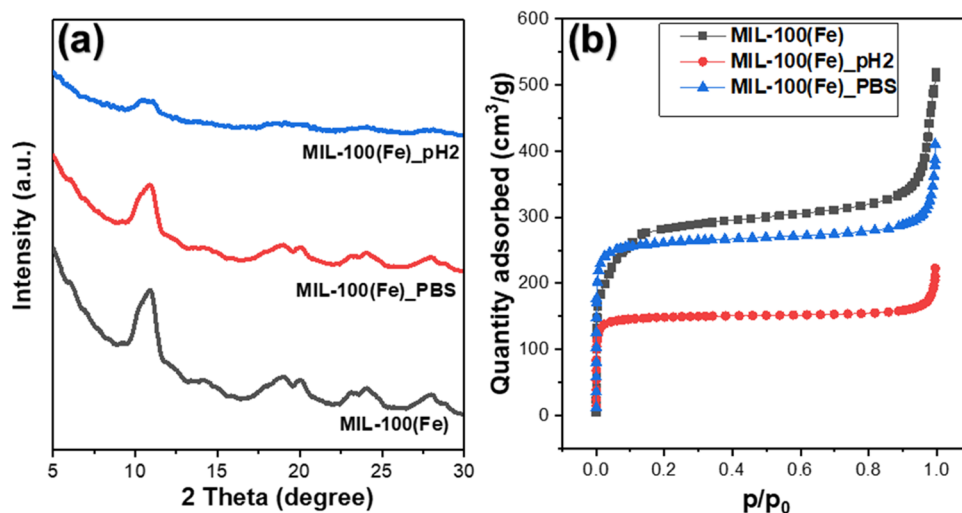
Figure 9. (a) XRD patterns and (b) nitrogen adsorption plots of initial MIL-100(Fe) and MIL-100(Fe) after releasing chloroquine drug in PBS and the pH 2 solutions.

compared to that of 1033.7 m^2/g of initial MIL-100(Fe) (Figure 9b).

The acute and 7 day oral toxicity studies were carried out to evaluate the toxicity of MIL-100(Fe) as shown in Figure 10. It
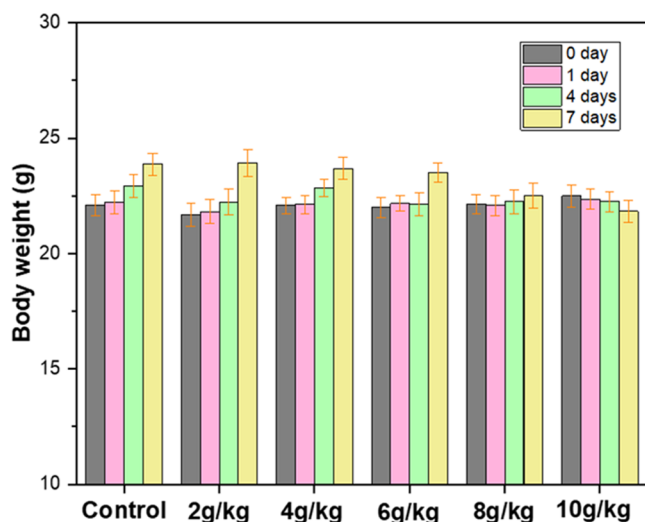

Figure 10. Change of body weight in mice treated with MIL-100(Fe) with various doses for 7 days.

can be clearly seen from Figure 10 that no toxicity of MIL-100(Fe) was observed in mice even at the high dose of 10 g/kg. All mice treated with the material were observed to behave normally without any toxic symptoms after observation for 3 days at the tested doses. The weight of the body, food, and water consumption of the mice administered with MIL-100(Fe) were similar to the control group. The MIL-100(Fe)-treated mice also respond normally to sound and light with no death during the testing period. Throughout the testing period, water and food uptake of the treated mice exhibited a negligible difference in and subchronic toxicity at all doses of MIL-100(Fe). However, at the dose of 10 g/kg, the mice group showed some clinical symptoms, for example, mild diarrhea in one male and two females. The body weights of the controlled groups were a little higher than that of the treated mice.

3. CONCLUSIONS

In summary, MIL-100(Fe) metal−organic frameworks were successfully synthesized by the ultrasonic method from the organic ligand and Fe ions. The prepared MIL-100(Fe) was of particle size in the range of 100−300 nm, with a specific surface area of up to 1033 m^2/g. The pore volume and pore diameter of the material were determined to be 0.764 cm^3/g and 2.96 nm, respectively. MIL-100(Fe) also contained functional groups on the surface as well as in the network, which are suitable for drug delivery. The resultant MIL-100(Fe) material revealed a high loading capacity for chloroquine with a maximal capacity of up to 22%. The analysis of the MIL-100(Fe)@chloroquine system showed that the material still retains its structure and granularity after chloroquine attachment. The change in surface area, as well as the appearance of some fluctuations in the structure, also proved the successful loading of the drug in the MIL-100(Fe) material. The MIL-100(Fe)@chloroquine system exhibited the slow release of the chloroquine molecules in PBS environment (pH 7.4) and simulated gastric (pH 2) environments. The MIL-100(Fe)@chloroquine system released approximately 80% of the drug after 7.5 h and only completely detached from the material after 80 h of immersion. The mice treated with the MIL-100(Fe) material showed no death or signs of changes in locomotor activities 7 days at all tested dose groups. With the high loading and slow release of the chloroquine drug, further studies should be conducted to evaluate the cytotoxicity and other biological factors to enable the utilization of the MIL-100(Fe) metal−organic framework for the controlled delivery of chloroquine drug.

4. EXPERIMENTAL SECTION

Materials. Ferric clorua hydrate (FeCl$_3$·6H$_2$O, 98%), trimesic acid (C$_6$H$_3$(COOH)$_3$, H$_3$BTC, 95%), chloroquine phosphate C$_{18}$H$_{26}$ClN$_3$·2H$_3$PO$_4$, ethanol, and phosphate-buffered saline tablet pH 7.4 (PBS) were obtained from Sigma-Aldrich. Deionized water was employed in all experimental processes. All chemicals were used without any further purification.

Synthesis of MIL-100(Fe). In a typical process, 2.7 g of FeCl$_3$·6H$_2$O and 1.4 g of 1,3,5 BTC: H$_2$O were introduced

into 100 mL of deionized water. The mixture was well-stirred for 15 min and then sonicated using a probe ultrasonic homogenizer for 10 min with a power of 1080 W and a frequency of 20.5 kHz. The precipitates obtained after the reaction was filtered and washed three times with ethanol and several times with deionized water. Finally, the product was dried at a temperature of 150 °C, followed by naturally cooling down to room temperature and storing for the next experiment.

Characterizations of the MIL-100(Fe) Material. MIL-100(Fe) morphology was observed on a scanning electron microscope (SEM) Hitachi S-4800. The chemical nature of the materials before and after chloroquine loading was studied by Raman spectroscopy (Thermo Scientific DXR3) and FTIR transform infrared spectroscopy (Perkin Elmer Spectrum 2). XRD pattern obtained on the X'Pert PRO instrument with a radiation source of 1.54060 Å Cu Kα was used to study the crystalline nature of the materials. The surface area and porous properties of MIL-100(Fe) before and after loading with chloroquine were evaluated by nitrogen isothermal adsorption obtained on TriStar II Plus instrument. Chloroquine concentration was determined using a UV−vis spectrophotometer (Drawell DU-8200).

Loading Kinetics, Drug Loading, and Release Experiment. The loading kinetics, loading capacity, and drug release efficiency were evaluated by measuring the concentration of chloroquine in the solution using UV−vis spectroscopy recorded at 329 nm. For the loading kinetics study, 0.5 g of the prepared MIL-100(Fe) material was immersed in 0.5 L of 100 ppm chloroquine solution. The mixture was shaken at a speed of 150 rpm at different periods. After a certain time, 50 mL of the mixture was taken out, the chloroquine-loaded MIL-100(Fe) material was filtered, and the UV−vis spectrum was measured to determine the remaining chloroquine in the solution. The experiments were repeated three times to determine the average values.

Determination of Loading Capacity. Various chloroquine concentrations of 90, 100, 200, 300, 400, 500, and 1000 ppm were prepared in deionized water. Then, the MIL-100(Fe) material was added to the chloroquine solutions with the ratio of 1 g of the MIL-100(Fe)/1 L chloroquine solution. The mixtures were shaken at the speed of 150 rpm for 10 days to reach chloroquine adsorption equilibrium. Each mixture was filtered to collect the loaded MIL-100(Fe) material and measured the UV−vis spectrum of the residual solution for the determination of the remaining chloroquine drug. The experiments were repeated three times to determine the average values.

Drug Release Behavior Testing of MIL-100(Fe)@Chloroquine System. The prepared MIL-100(Fe)@chloroquine was separately immersed in the PBS and simulated gastric (pH of 2) solution with the concentration of 1 g/L at the body-simulated temperature of 37 °C. Certain volumes of solution were taken out at designed time points to measure chloroquine concentrations released from the chloroquine-loaded MIL-100(Fe) material. The experiments were repeated three times to determine the average values.

■ ASSOCIATED CONTENT

ⓢ Supporting Information

The Supporting Information is available free of charge at https://pubs.acs.org/doi/10.1021/acsomega.2c06676.

This provides further information about the XRD pattern of the MIL-100(Fe) metal−organic frameworks (PDF)

■ AUTHOR INFORMATION

Corresponding Author

Phuong Thi Hoai Nguyen − *Institute of Chemistry and Materials, Hanoi 100000, Vietnam*;
  Email: hoaiphuong1978@gmail.com

Authors

Bac Thanh Le − *Institute of Chemistry and Materials, Hanoi 100000, Vietnam*

Duong Duc La − *Institute of Chemistry and Materials, Hanoi 100000, Vietnam*; ⓞ orcid.org/0000-0003-4241-4431

Complete contact information is available at:
https://pubs.acs.org/10.1021/acsomega.2c06676

Author Contributions

The manuscript was written through the contributions of all authors. All authors have approved the final version of the manuscript.

Notes

The authors declare no competing financial interest.

■ ACKNOWLEDGMENTS

■ REFERENCES

(1) Férey, G. Hybrid porous solids: past, present, future. *Chem. Soc. Rev.* **2008**, *37*, 191−214.

(2) Lee, J.; Farha, O. K.; Roberts, J.; Scheidt, K. A.; Nguyen, S. T.; Hupp, J. T. Metal−organic framework materials as catalysts. *Chem. Soc. Rev.* **2009**, *38*, 1450−1459.

(3) Yanturali, S.; Aksay, E.; Demir, O.; Atilla, R. Massive hydroxychloroquine overdose. *Acta Anaesthesiol. Scand.* **2004**, *48*, 379−381.

(4) Guo, Y.; Yan, B.; Cheng, Y.; Mu, L. A new Dy (III)-based metal-organic framework with polar pores for pH-controlled anticancer drug delivery and inhibiting human osteosarcoma cells. *J. Coord. Chem.* **2019**, *72*, 262−271.

(5) Liang, Y.; Huang, H.; Kou, L.; Li, F.; Lu, J.; Cao, H. L. Synthesis of Metal−Organic Framework Materials by Reflux: A Faster and Greener Pathway to Achieve Super-Hydrophobicity and Photo-catalytic Application. *Cryst. Growth Des.* **2018**, *18*, 6609−6616.

(6) Nivetha, R.; Gothandapani, K.; Raghavan, V.; Jacob, G.; Sellappan, R.; Bhardwaj, P.; Pitchaimuthu, S.; Kannan, A. N. M.; Jeong, S. K.; Grace, A. N. Highly Porous MIL-100 (Fe) for the Hydrogen Evolution Reaction (HER) in Acidic and Basic Media. *ACS Omega* **2020**, *5*, 18941−18949.

(7) Simon, M. A.; Anggraeni, E.; Soetaredjo, F. E.; Santoso, S. P.; Irawaty, W.; Thanh, T. C.; Hartono, S. B.; Yuliana, M.; Ismadji, S. Hydrothermal synthesize of HF-free MIL-100 (Fe) for isoniazid-drug delivery. *Sci. Rep.* **2019**, *9*, No. 16907.

(8) Zhong, G.; Liu, D.; Zhang, J. Applications of Porous Metal−Organic Framework MIL-100 (M)(M = Cr, Fe, Sc, Al, V). *Cryst. Growth Des.* **2018**, *18*, 7730−7744.

(9) Alhumaimess, M. S. Metal−Organic Frameworks and their Catalytic Applications. *J. Saudi Chem. Soc.* **2020**, *24*, 461−473.

(10) Almáši, M.; Zeleňák, V.; Palotai, P.; Beňová, E.; Zeleňáková, A. Metal-organic framework MIL-101 (Fe)-NH2 functionalized with

different long-chain polyamines as drug delivery system. *Inorg. Chem. Commun.* **2018**, *93*, 115−120.

(11) Della Rocca, J.; Liu, D.; Lin, W. Nanoscale metal−organic frameworks for biomedical imaging and drug delivery. *Acc. Chem. Res.* **2011**, *44*, 957−968.

(12) Horcajada, P.; Serre, C.; Maurin, G.; Ramsahye, N.; Balas, M. A.; V -R, M.; Sebban; Taulelle, F.; Férey, G. R. Flexible Porous Metal-Organic Frameworks for a Controlled Drug Delivery. *J. Am. Chem. Soc* **2008**, *130*, 6774−6780.

(13) Javanbakht, S.; Pooresmaeil, M.; Namazi, H. Green one-pot synthesis of carboxymethylcellulose/Zn-based metal-organic framework/graphene oxide bio-nanocomposite as a nanocarrier for drug delivery system. *Carbohydr. Polym.* **2019**, *208*, 294−301.

(14) McKinlay, A. C.; Morris, R. E.; Horcajada, P.; Férey, G.; Gref, R.; Couvreur, P.; Serre, C. BioMOFs: metal−organic frameworks for biological and medical applications. *Angew. Chem., Int. Ed.* **2010**, *49*, 6260−6266.

(15) Horcajada, P.; Chalati, T.; Serre, C.; Gillet, B.; Sebrie, C.; Baati, T.; Eubank, J. F.; Heurtaux, D.; Clayette, P.; Kreuz, C. Porous metal−organic-framework nanoscale carriers as a potential platform for drug delivery and imaging. *Nat. Mater.* **2010**, *9*, 172−178.

(16) Miller, S. R.; Heurtaux, D.; Baati, T.; Horcajada, P.; Grenèche, J.-M.; Serre, C. Biodegradable therapeutic MOFs for the delivery of bioactive molecules. *Chem. Commun.* **2010**, *46*, 4526−4528.

(17) Nguyen Thi, H. P.; Ninh, H. D.; Van Tran, C.; Le, B. T.; Bhosale, S. V.; Duc, L. D. Size-Control and Surface Modification of Flexible Metal-Organic Framework MIL-53 (Fe) by Polyethyleneglycol for 5-Fluorouracil Anticancer Drug Delivery. *ChemistrySelect* **2019**, *4*, 2333−2338.

(18) Simon-Yarza, T.; Baati, T.; Neffati, F.; Njim, L.; Couvreur, P.; Serre, C.; Gref, R.; Najjar, M. F.; Zakhama, A.; Horcajada, P. In vivo behavior of MIL-100 nanoparticles at early times after intravenous administration. *Int. J. Pharm.* **2016**, *511*, 1042−1047.

(19) Márquez, A. G.; Demessence, A.; Platero-Prats, A. E.; Heurtaux, D.; Horcajada, P.; Serre, C.; Chang, J. S.; Férey, G.; de la Peña-O'Shea, V. A.; Boissière, C. Green Microwave Synthesis of MIL-100 (Al, Cr, Fe) Nanoparticles for Thin-Film Elaboration. *Eur. J. Inorg. Chem.* **2012**, *2012*, 5165−5174.

(20) Gecgel, C.; Simsek, U. B.; Gozmen, B.; Turabik, M. Comparison of MIL-101 (Fe) and amine-functionalized MIL-101 (Fe) as photocatalysts for the removal of imidacloprid in aqueous solution. *J. Iran. Chem. Soc.* **2019**, *16*, 1735−1748.

(21) Jeremias, F.; Henninger, S. K.; Janiak, C. Ambient pressure synthesis of MIL-100 (Fe) MOF from homogeneous solution using a redox pathway. *Dalton Trans.* **2016**, *45*, 8637−8644.

(22) Jhung, S. H.; Lee, J. H.; Yoon, J. W.; Serre, C.; Férey, G.; Chang, J. S. Microwave synthesis of chromium terephthalate MIL-101 and its benzene sorption ability. *Adv. Mater.* **2007**, *19*, 121−124.

(23) Shi, J.; Hei, S.; Liu, H.; Fu, Y.; Zhang, F.; Zhong, Y.; Zhu, W. Synthesis of MIL-100 (Fe) at low temperature and atmospheric pressure. *J. Chem.* **2013**, *2013*, No. 792827.

(24) Tilley, L.; Davis, T. M.; Bray, P. G. Prospects for the treatment of drug-resistant malaria parasites. *Future Microbiol.* **2006**, *1*, 127−141.

(25) Browning, D. J. *Hydroxychloroquine and Chloroquine Retinopathy*; Springer, 2014.

(26) Cortegiani, A.; Ingoglia, G.; Ippolito, M.; Giarratano, A.; Einav, S. A systematic review on the efficacy and safety of chloroquine for the treatment of COVID-19. *J. Crit. Care* **2020**, *57*, 279−283.

(27) Liu, J.; Cao, R.; Xu, M.; Wang, X.; Zhang, H.; Hu, H.; Li, Y.; Hu, Z.; Zhong, W.; Wang, M. Hydroxychloroquine, a less toxic derivative of chloroquine, is effective in inhibiting SARS-CoV-2 infection in vitro. *Cell Discovery* **2020**, *6*, No. 16.

(28) Furst, D. E. Pharmacokinetics of hydroxychloroquine and chloroquine during treatment of rheumatic diseases. *Lupus* **1996**, *5*, 11−15.

(29) Marquardt, K.; Albertson, T. E. Treatment of hydroxychloroquine overdose. *Am. J. Emerg. Med.* **2001**, *19*, 420−424.

(30) Pelt, J.; Busatto, S.; Ferrari, M.; Thompson, E. A.; Mody, K.; Wolfram, J. Chloroquine and nanoparticle drug delivery: A promising combination. *Pharmacol. Ther.* **2018**, *191*, 43−49.

(31) Tripathy, S.; Das, S.; Chakraborty, S. P.; Sahu, S. K.; Pramanik, P.; Roy, S. Synthesis, characterization of chitosan−tripolyphosphate conjugated chloroquine nanoparticle and its in vivo anti-malarial efficacy against rodent parasite: A dose and duration dependent approach. *Int. J. Pharm.* **2012**, *434*, 292−305.

(32) Zhang, X.; Zeng, X.; Liang, X.; Yang, Y.; Li, X.; Chen, H.; Huang, L.; Mei, L.; Feng, S.-S. The chemotherapeutic potential of PEG-b-PLGA copolymer micelles that combine chloroquine as autophagy inhibitor and docetaxel as an anti-cancer drug. *Biomaterials* **2014**, *35*, 9144−9154.

(33) Raju, G. S. R.; Pavitra, E.; Merchant, N.; Lee, H.; Prasad, G. L. V.; Nagaraju, G. P.; Huh, Y. S.; Han, Y.-K. Targeting autophagy in gastrointestinal malignancy by using nanomaterials as drug delivery systems. *Cancer Lett.* **2018**, *419*, 222−232.

(34) Mallakpour, S.; Nikkhoo, E.; Hussain, C. M. Application of MOF materials as drug delivery systems for cancer therapy and dermal treatment. *Coord. Chem. Rev.* **2022**, *451*, No. 214262.

(35) Pourmadadi, M.; Eshaghi, M. M.; Ostovar, S.; Shamsabadipour, A.; Safakhah, S.; Mousavi, M. S.; Rahdar, A.; Pandey, S. UiO-66 metal-organic framework nanoparticles as gifted MOFs to the biomedical application: A comprehensive review. *J. Drug Delivery Sci. Technol.* **2022**, *76*, No. 103758.

(36) Yalamandala, B. N.; Shen, W. T.; Min, S. H.; Chiang, W. H.; Chang, S. J.; Hu, S. H. Advances in Functional Metal-Organic Frameworks Based On-Demand Drug Delivery Systems for Tumor Therapeutics. *Adv. NanoBiomed Res.* **2021**, *1*, No. 2100014.

(37) Linnane, E.; Fairen-Jimenez, D. Metal-Organic Frameworks as Delivery Systems of Small Drugs and Biological Gases. In *Metal-Organic Frameworks in Biomedical and Environmental Field*; Springer, 2021; pp 349−378.

(38) Shi, Z.; Chen, X.; Zhang, L.; Ding, S.; Wang, X.; Lei, Q.; Fang, W. FA-PEG decorated MOF nanoparticles as a targeted drug delivery system for controlled release of an autophagy inhibitor. *Biomater. Sci.* **2018**, *6*, 2582−2590.

(39) Jodłowski, P. J.; Kurowski, G.; Kuterasiński, Ł.; Sitarz, M.; Jeleń, P.; Jaśkowska, J.; Kołodziej, A.; Pajdak, A.; Majka, Z.; Boguszewska-Czubara, A. Cracking the Chloroquine Conundrum: The Application of Defective UiO-66 Metal−Organic Framework Materials to Prevent the Onset of Heart Defects—In Vivo and In Vitro. *ACS Appl. Mater. Interfaces* **2020**, *13*, 312−323.

(40) Zhang, L.; Tian, J.; Cao, F.; Zhu, Z.-Y.; Hong, F.; Wu, J.; Wang, F. Titanium-based metal−organic frameworks as potential chloroquine drug carriers. *Inorg. Chem. Commun.* **2021**, *133*, No. 108870.

(41) Huang, S.; Yang, K.-L.; Liu, X.-F.; Pan, H.; Zhang, H.; Yang, S. MIL-100 (Fe)-catalyzed efficient conversion of hexoses to lactic acid. *RSC Adv.* **2017**, *7*, 5621−5627.

(42) Yang, J.; Niu, X.; An, S.; Chen, W.; Wang, J.; Liu, W. Facile synthesis of Bi 2 MoO 6−MIL-100 (Fe) metal−organic framework composites with enhanced photocatalytic performance. *RSC Adv.* **2017**, *7*, 2943−2952.

(43) Mahmoudi, F.; Amini, M. M.; Sillanpää, M. Hydrothermal synthesis of novel MIL-100 (Fe)@ SBA-15 composite material with high adsorption efficiency towards dye pollutants for wastewater remediation. *J. Taiwan Inst. Chem. Eng.* **2020**, *116*, 303−313.

(44) Souza, B. E.; Möslein, A. F.; Titov, K.; Taylor, J. D.; Rudic, S.; Tan, J.-C. Green reconstruction of MIL-100 (Fe) in water for high crystallinity and enhanced guest encapsulation. *ACS Sustainable Chem. Eng.* **2020**, *8*, 8247−8255.

(45) Seo, Y.-K.; Yoon, J. W.; Lee, J. S.; Lee, U.-H.; Hwang, Y. K.; Jun, C.-H.; Horcajada, P.; Serre, C.; Chang, J.-S. Large scale fluorine-free synthesis of hierarchically porous iron (III) trimesate MIL-100 (Fe) with a zeolite MTN topology. *Microporous Mesoporous Mater.* **2012**, *157*, 137−145.

(46) Leclerc, H.; Vimont, A.; Lavalley, J.-C.; Daturi, M.; Wiersum, A. D.; Llewellyn, P. L.; Horcajada, P.; Férey, G.; Serre, C. Infrared study of the influence of reducible iron (III) metal sites on the adsorption of

CO, CO 2, propane, propene and propyne in the mesoporous metal—organic framework MIL-100. *Phys. Chem. Chem. Phys.* **2011**, *13*, 11748−11756.

(47) Lestari, W. W.; Yunita, L.; Saraswati, T. E.; Heraldy, E.; Khafidhin, M. A.; Krisnandi, Y. K.; Arrozi, U. S. F.; Kadja, G. Fabrication of composite materials MIL-100 (Fe)/Indonesian activated natural zeolite as enhanced CO2 capture material. *Chem. Pap.* **2021**, *75*, 3253−3263.

(48) Li, X.; Lachmanski, L.; Safi, S.; Sene, S.; Serre, C.; Grenèche, J.-M.; Zhang, J.; Gref, R. New insights into the degradation mechanism of metal-organic frameworks drug carriers. *Sci. Rep.* **2017**, *7*, No. 13142.

(49) Saafan, H. A.; Ibrahim, K. M.; Thabet, Y.; Elbeltagy, S. M.; Eissa, R. A.; Ghaleb, A. H.; Ibrahim, F.; Elsabahy, M.; Eissa, N. G. Intratracheal administration of chloroquine-loaded niosomes minimize systemic drug exposure. *Pharmaceutics* **2021**, *13*, No. 1677.